Switchable Fluorescent Imaging of Intracellular Telomerase Activity Using Telomerase-Responsive Mesoporous Silica Nanoparticle

Ruocan Qian,[†] Lin Ding,[†] and Huangxian Ju*

State Key Laboratory of Analytical Chemistry for Life Science, School of Chemistry and Chemical Engineering, Nanjing University, Nanjing 210093, P.R. China

S Supporting Information

ABSTRACT: This work designs a telomerase-responsive mesoporous silica nanoparticle (MSN) to realize in situ "off-on" imaging of intracellular telomerase activity. In the wrapping DNA (O1) sealed MSN probe, a black hole fluorescence quencher is covalently immobilized on the inner walls of the mesopores, while fluorescein is loaded in the mesopores. In the presence of telomerase and dNTPs, the designed O1 can be extended and then moves away from the MSN surface via forming a rigid hairpin-like DNA structure. Thus the O1 can act as a "biogate" to block and release fluorescein for "off-on" switchable fluorescent imaging. The MSN probe exhibits good performance for sensitive in situ tracking of telomerase activity in living cells. The practicality of this protocol has been verified by monitoring the change of cellular telomerase activity in response to telomerase-related drugs.

Human telomerase is a ribonucleoprotein reverse transcriptase adding repeated DNA sequence TTAGGG to the 3′ end of telomeres.[1−3] In normal cells, as the telomerase expression is repressed or absent, telomeres are progressively shortened during each round of cell division. After their length reaches thresholds, the cells stop dividing and reach the senescent phase.[4] In cancer cells the overexpressed telomerase can maintain the length of telomeres,[5] leading to unlimited cellular proliferation.[6,7] Therefore, the analysis, particularly in situ monitoring, of telomerase activity, is significant to cancer diagnosis, therapy, and monitoring.[8]

Currently, a variety of methods have been used to probe telomerase activity.[9] The most common method is polymerase chain reaction (PCR)-based telomeric repeat amplification protocol.[10] This method suffers from the shortcoming of the inhibition of polymerase in clinical samples.[7,11] Therefore, alternative PCR-free methods have been actively developed, including biocatalytic precipitation-based electrochemical methods,[12] optical detection using DNA beacons[13] or two-color coincidence,[14] nanosensors,[15,16] biobarcode technique,[17,18] and magnetic bead-based electrochemiluminescent detection,[19] etc. These works use cell extract for telomerase activity analysis, thus failing to in situ detect and provide telomerase information at single-cell levels. Although the visualization of human telomerase reverse transcriptase promoter fragments[20] or mRNA[21] in single cells has been achieved, these technologies cannot directly reflect the telomerase activity. Thus, in situ

detection protocol for monitoring intracellular telomerase activity has become an urgent need.

Nanomaterials have showed their powerful ability to construct delivery platforms for intracellular research.[9,22] Mesoporous silica nanoparticle (MSN) is especially attractive due to its unique pore structure, biocompatibility, and ease of functionalization.[23,24] Particularly, the large pore volume and surface area of MSN make it possible to load large numbers of molecules.[25] Thus this nanomaterial has been used as carrier of pH,[26] redox potential,[27] light,[28] and DNA-responsive[23] probes for controlled release. This work used MSN to assemble a specially designed wrapping DNA (O1) as a biogate for the design of a telomerase-responsive probe. The in situ synthesis of telomeric repeats at the 3′ end of O1 led to the detachment of O1 from the probe surface (Scheme 1). By entrapping fluorescein in the mesopores of MSN and covalently immobilizing black hole fluorescence quencher (BHQ) on

Scheme 1. Schematic Illustration of MSN Probe-Based Intracellular Analysis of Telomerase

Telomerase mediated O1 extension, detachment & fluorescein release
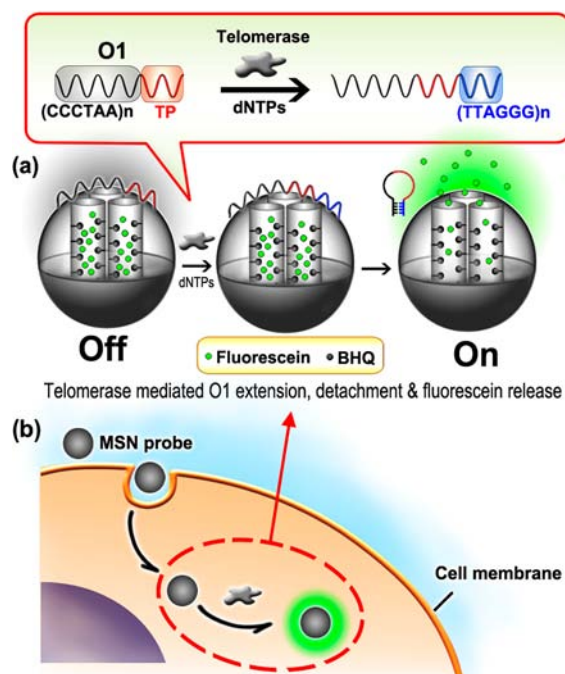
the inner walls of the mesopores, the detachment of O1 triggered the release of fluorescein, thus turned "on" its fluorescence. This switchable probe provided a powerful protocol for "off-on" fluorescent imaging of intracellular telomerase activity.

The sequence of O1 was 5′-(CCCTAA)$_n$AATCCG TCGAGC AGAGTT-3′. Here the underlined part was the telomerase primer (TP). In the absence of telomerase, the O1 sealed MSN probe was at its "off" state due to the quenching effect of the immobilized BHQ to the fluorescence fluorescein. When the probe met telomerase, the O1 could be extended in the presence of dNTPs, producing telomeric repeated sequence at its 3′ end, which was just complementary with its 5′ end. The hybridization of the complementary sequences at 5′ and 3′ ends produced a rigid hairpin-like DNA structure and led to the detachment of the extended O1 from MSN and the release of the entrapped fluorescein to turn "on" the fluorescence (Scheme 1a). Using human cervical cells (HeLa) as a model, MSN probe could be used as an intracellular delivery vehicle. After MSN probe was taken in by cells, the fluorescence could be activated with the action of intracellular telomerase (Scheme 1b). Through observation of the fluorescence signal, the in situ tracking of intracellular telomerase activity could be achieved, leading to a facile strategy for monitoring the change of cellular telomerase activity in response to drugs. Compared with existing methods using cell extracts for telomerase detection, this work realized the convenient in situ imaging of telomerase activity in living cells.

MSN was synthesized by a modified sol−gel procedure (Supporting Information, SI).[23,29] The nitrogen adsorption−desorption isotherm indicated that MSN was porous with a 2 nm average pore diameter (Figure 1a). Dynamic light scattering (DLS) experiment showed an average hydration diameter ∼180 nm with a uniform distribution (Figure 1b). The porosity and dimension of MSN reflected by transmission electron microscopic (TEM) images were in good agreement with these data (Figure 1c). After MSN was modified with 3-aminopropyl-triethoxysilane (APTES) to present aminopropyl groups on the wall of mesopores,[23] BHQ could be covalently linked to the wall. The MSN was then loaded with fluorescein to produce fluorescein@MSN-BHQ, which was further wrapped by O1 to obtain MSN probe (SI). Zeta-potential analysis indicated that
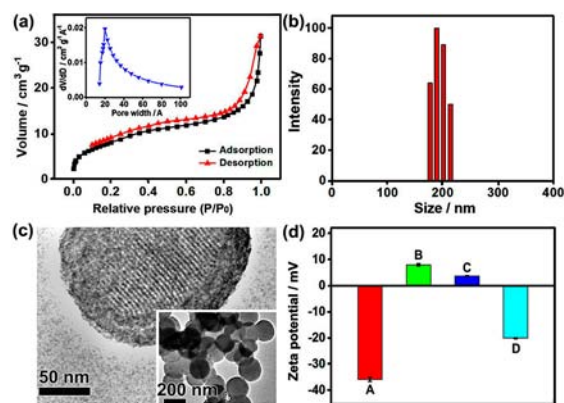
after APTES modification, the MSN became positively charged, and the covalent linkage of BHQ followed with entrapping of fluorescein slightly decreased the positive charge (Figure 1d). The positively charged fluorescein@MSN-BHQ was demonstrated to be beneficial for electrostatic adsorption of the negatively charged O1 (Figure S1). The attachment of O1 produced a negatively charged MSN probe.

MSN probe (dispersed in HB) displayed negligible fluorescence, while the fluorescence of the fluorescein@MSN-BHQ without O1 wrap became greater with an increasing time due to the release of fluorescein from the mesopores (Figure S2a,b), demonstrating the blocking function of O1. The amount of fluorescein loaded in MSN probe was determined to be 4.0 mg g^{-1} MSN (Figure S3), indicating the high loading capability of MSN due to its unique mesoporous structure. O2, the complementary strand of O1, was used to test the "biogate". As predicted, upon incubation of MSN probe with O2, gradual release of fluorescein was observed, which reached a maximum value after 80 min (Figure S2c), slightly later than 60 min of fluorescein@MSN-BHQ, demonstrating the hybridization-induced detachment of O1. This phenomenon was also observed by detecting the fluorescence change of fluorescein-labeled O1 wrapped APTES-modified MSN-BHQ upon incubation with O2 (Figure S1a). To exclude the interference of MSN, after incubating MSN probe with O2 for different times, the supernatants were collected for fluorescent detection, which showed the same tendency as that without separation of MSN (Figure S2d). Moreover, O1 sealed MSN probe could keep the controllable release feature and good particle stability in different media (Figure S4), in which both the releasing tendency and the particle size were similar to those in HB.

For evaluation of the telomerase-responsive release mechanism, MSN probe was incubated with telomerase and dNTPs for different times, and the supernatants were subjected to fluorescent and UV−vis analysis (Supporting Information). A gradual increase of fluorescein intensity with an increasing incubation time was observed, and the fluorescent signal reached the maximum value after 90 min (Figure 2a), demonstrating the telomerase-induced release of fluorescein. The extension of O1 caused by telomerase could be verified by gel electrophoresis (Supporting Information). After incubating MSN probe with telomerase and dNTPs for 1 h, the supernatant showed an extended product of 70 bp (lane C in Figure 2b), which was about 3 TTTGGG segments longer than O1 (lane A in Figure 2b), and the corresponding UV−vis spectrum showed a characteristic peak for DNA at 260 nm (Figure 2c). Thus the UV−vis spectra could be used to detect the concentrations of the detached DNA at different incubation times. From the plot of the detached DNA concentration vs reaction time (Figure S5a), the reaction rate at each time point could be obtained. The reaction rate was proportional to the concentration of O1 as the substrate of telomerase (Figure S5b), indicating a pseudo-first-order telomerase-catalyzed reaction with the rate constant to be ∼0.023 min^{-1}.

To verify the specificity of MSN probe to telomerase, a control DNA, 5′-(TTTTTT)$_9$-3′(O3), was employed to replace O1. After incubating O3 wrapped fluorescein@MSN-BHQ with telomerase and dNTPs at different times, the supernatants showed much lower fluorescence intensity than those of the MSN probe, indicating negligible fluorescein release (Figure S6) and that telomerase could recognize and open only the biogate designed with O1. Above results demonstrated the telomerase-responsive controlled-release
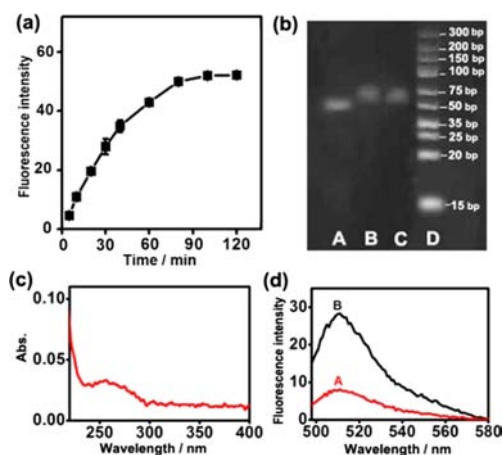

Figure 1. (a) Nitrogen adsorption−desorption isotherm of MSN. Inset: pore size distribution. (b) DLS characterization of MSN. (c) TEM images of MSN. (d) Zeta-potentials of (A) MSN, (B) APTES-MSN, (C) fluorescein@MSN-BHQ, and (D) MSN probe (1 mg mL^{-1}) in hybridization buffer (HB).

Figure 2. (a) Plot of fluorescence intensity of the supernatant collected after incubating MSN probe with telomerase and dNTPs vs incubation time. (b) Electrophoresis image of (A) O1, (B) supernatant collected after incubating MSN probe with dNTPs and cell extract, or (C) pure telomerase for 1 h, and (D) ladder DNA. (c) UV−vis spectrum of the supernatant collected after incubating MSN probe with telomerase and dNTPs for 1h. (d) Fluorescence spectra of the supernatant collected after incubating MSN probe with (A) dNTPs and cell extract and with (B) dNTPs and pure telomerase spiked in cell extract for 1 h.

Figure 3. (a) Time course of confocal image of HeLa cells incubated with 15 μL MSN probe (1 mg mL⁻¹). (b) and (c) TEM images of MSN internalized HeLa cells at two amplifications.

mechanism and the feasibility of specific "off-on" detection of the telomerase activity.

Since telomerase was overexpressed in cancer cells, the cell extract from HeLa cells was used for opening the biogate. The resistance ability of MSN probe against nuclease cleavage and single-stranded DNA binding protein (SSB) in HB and acidic PBS was first examined, which showed little fluorescein release (Figure S7),[30] demonstrating the protective ability of MSN against proteins coexisting in cell extract and acidic subcellular environment. After the MSN probe was incubated with dNTPs and cell extract for 1 h, the collected supernatant showed an obvious electrophoresis band at the same position as the telomerase-induced extension product of O1 (lane B in Figure 2b) and fluorescent spectrum of fluorescein (curve A in Figure 2d), verifying the presence of telomerase in cell extract to trigger the extension and detachment of O1. From the fluorescent spectrum the activity of telomerase in the cell extract from 1×10^6 HeLa cells was detected to be 3.1×10^{-5} IU with a standard addition method (curve B in Figure 2d).

After treating with the MSN probe for 3 h, the HeLa cells still maintained about 90.2% of the cell viability (Figure S8), indicating low cytotoxicity of MSN probe. For in situ imaging, HeLa cells (0.5 mL, 1×10^6 mL⁻¹) were cultured in a 20 mm confocal dish for 24 h, and 15 μL MSN probe (1 mg mL⁻¹) was then added in the dish to observe the fluorescence. Upon addition of MSN probe, the cells did not show detectable fluorescence within initial 30 min. After 50 min, fluorescence emerged in the cytoplasm, and its intensity gradually increased due to the release of fluorescein (Figure 3a). The fluorescence intensity reached the maximum at 90 min. The confocal microscopic images indicated that the fluorescence spots mainly distributed in the cytoplasm nearby the nucleus, where telomerase possesses high activity.[31] The internalization and localization of MSN probe in cytoplasm were also observed from the TEM images (Figure 3b,c). The endocytosis regardless of cell types sharply depended on the temperature,
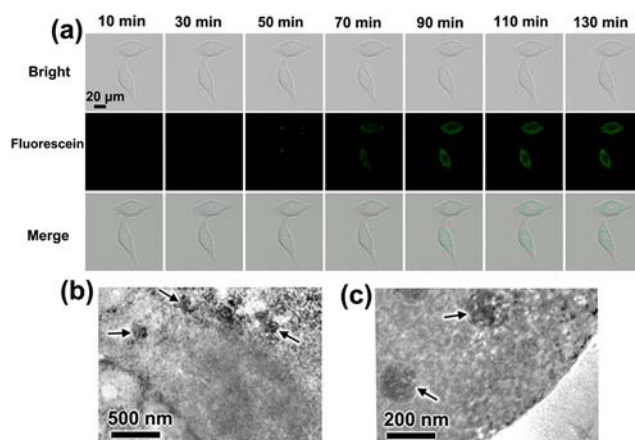
suggesting an energy-dependent endocytosis of the MSN probe (Figure S9).[32]

Flow cytometry was also used to evaluate the release of fluorescein mediated by telomerase in the cytoplasm. Under the same incubation condition, the fluorescence intensity within HeLa cells increased with the increasing incubation time and reached a plateau at 1.5 h (Figure S10), which was in agreement with the confocal microscopic results. For sensitively detecting the cellular telomerase activity, the amount of MSN probe (1 mg mL⁻¹) was optimized with flow cytometry to be 15 μL (Figure S11).

To demonstrate the specificity of the MSN probe for telomerase activity detection in living cells, O3 wrapped fluorescein@MSN-BHQ was used to perform the same test. After incubation for 1.5 h, little fluorescence could be observed (Figure S12a), demonstrating the specific recognition of telomerase to the designed O1, which was further verified by flow cytometric detection (Figure S12b).

The feasibility of the MSN probe for other cell lines was demonstrated using BEL-7402 cells (liver cancer cells) and QSG-7701 cells (liver normal cells) as the models. Greater telomerase activity in cancer cells compared with normal cells was observed (Figure S13a), which was further verified by flow cytometric detection (Figure S13b). Thus the designed strategy could be applied for various cell types and distinguishing cancer cells from normal cells.

The MSN probe was further employed for in situ monitoring the change of cellular telomerase activity after treated with drugs. Telomerase sense oligodeoxynucleotide (SODN), telomerase antisense oligodeoxynucleotide (ASODN), and epigallocatechingallate (EGCG) were used as model drugs to study the telomerase-inhibition effect in HeLa cells. After HeLa cells (0.5 mL, 1×10^6 mL⁻¹) were cultured with 60 μL SODN (10 μM), 60 μL ASODN (10 μM), or 125 μg EGCG in confocal dish for 48 h, 15 μL MSN probe (1 mg mL⁻¹) was added to the dish and incubated for 1.5 h to observe the confocal image. The fluorescence intensity of SODN and ASODN treated cells obviously decreased, and the fluorescence of EGCG treated cells completely disappeared (Figure 4), which was in good agreement with flow cytometric results (Figure S14). Therefore, EGCG exhibited the most efficient inhibition for telomerase.
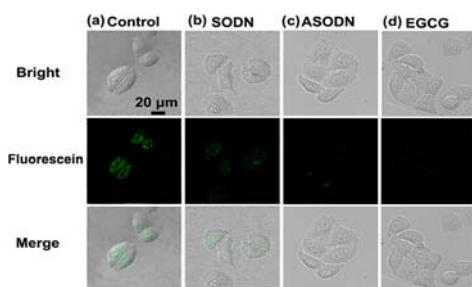
Figure 4. Confocal images of (a) control HeLa cells and HeLa cells pretreated with (b) SODN, (c) ASODN; and (d) EGCG after incubation with 15 μL MSN probe (1 mg mL^{-1}) for 1.5 h.

To obtain the calibration curve for quantification of intracellular telomerase activity, HeLa cells treated with different amounts of EGCG were subjected to telomerase kit detection. The plot of fluorescence intensity obtained from the confocal images of EGCG and then MSN probe treated cells vs the telomerase activity obtained from telomerase kit showed a linear relationship (Figure S15), leading to a noninvasive quantification method for intracellular telomerase activity. The telomerase activity was estimated to be 3.0×10^{-5}, 2.0×10^{-5}, and 8.0×10^{-7} IU for 1×10^6 HeLa, BEL, and QSG cells, respectively.

In conclusion, a DNA-based biogate was fabricated on MSN surface to produce a novel telomerase-responsive off-on fluorescent probe for switchable fluorescent detection of telomerase activity. This probe realized in situ tracking of intracellular telomerase activity with good performance and could distinguish various cells with different levels of telomerase activity. The proposed strategy could be employed for monitoring the change of intracellular telomerase activity in response to telomerase-based drugs. We anticipate that this strategy will accelerate the understanding of the biological roles of telomerase in cancer and provide a valuable tool for in vivo clinical diagnostics and discovery of novel telomerase-based drugs.

■ ASSOCIATED CONTENT

Ⓢ Supporting Information
Experimental details and figures. This material is available free of charge via the Internet at http://pubs.acs.org.

■ AUTHOR INFORMATION

Corresponding Author
E-mail:hxju@nju.edu.cn

Author Contributions
[†]These authors contributed equally to this work.

Notes
The authors declare no competing financial interest.

■ ACKNOWLEDGMENTS

■ REFERENCES

(1) Nakamura, T. M.; Morin, G. B.; Chapman, K. B.; Weinrich, S. L.; Andrews, W. H.; Lingner, J.; Harley, C. B.; Cech, T. R. *Science* **1997**, *277*, 955.

(2) Hammond, P. W.; Cech, T. R. *Nucleic Acids Res.* **1997**, *25*, 3698.
(3) Li, Y.; Liu, B. W.; Li, X.; Wei, Q. L. *Biosens. Bioelectron.* **2010**, *25*, 2543.
(4) Rodier, F.; Campisi, J. *J. Cell Biol.* **2011**, *192*, 547.
(5) Shay, J. W.; Bacchetti, S. *Eur. J. Cancer* **1997**, *33*, 787.
(6) Hahn, W. C.; Counter, C. M.; Lundberg, A. S.; Beijersbergen, R. L.; Brooks, M. W.; Weinberg, R. A. *Nature* **1999**, *400*, 464.
(7) Zhou, X. M.; Xing, D.; Zhu, D. B.; Jia, L. *Anal. Chem.* **2009**, *81*, 255.
(8) Hiyama, E.; Hiyama, K. *Oncogene* **2002**, *21*, 643.
(9) Zhou, X. M.; Xing, D. *Chem. Soc. Rev.* **2012**, *41*, 4643.
(10) Kim, N. W.; Piatyszck, M. A.; Prowse, K. R.; Harley, C. B.; West, M. D.; Ho, P. L.; Coviello, G. M.; Wright, W. E.; Weinrich, S. L.; Shay, J. W. *Science* **1994**, *266*, 2011.
(11) Kim, N. W.; Wu, F. *Nucleic Acids Res.* **1997**, *25*, 2595.
(12) Pavlov, V.; Willner, I.; Dishon, A.; Kotler, M. *Biosens. Bioelectron.* **2004**, *20*, 1011.
(13) Xiao, Y.; Pavlov, V.; Niazov, T.; Dishon, A.; Kotler, M.; Willner, I. *J. Am. Chem. Soc.* **2004**, *126*, 7430.
(14) Alves, D.; Li, H. T.; Codrington, R.; Ortel, A.; Ren, X. J.; Klenerman, D.; Balasubramanian, S. *Nat. Chem. Biol.* **2008**, *4*, 287.
(15) Niazov, T.; Pavlov, V.; Xiao, Y.; Gill, R.; Willner, I. *Nano Lett.* **2004**, *4*, 1683.
(16) Grimm, J.; Perez, J. M.; Josephson, L.; Weissleder, R. *Cancer Res.* **2004**, *64*, 639.
(17) Nam, J. M.; Wise, A. R.; Groves, J. T. *Anal. Chem.* **2005**, *77*, 6985.
(18) Zhu, D. B.; Tang, Y. B.; Xing, D.; Chen, W. *Anal. Chem.* **2008**, *80*, 3566.
(19) Zhou, X. M.; Xing, D.; Zhu, D. B.; Jia, L. *Anal. Chem.* **2009**, *81*, 255.
(20) Yu, S. T.; Li, C.; Lu, M. H.; Liang, G. P.; Li, N.; Tang, X. D.; Wu, Y. Y.; Shi, C. M.; Chen, L.; Li, C. Z.; Cao, Y. L.; Fang, D. C.; Yang, S. M. *Cancer* **2012**, *118*, 1884.
(21) Liu, M.; Wang, R. F.; Zhang, C. L.; Yan, P.; Yu, M. M.; Di, L. J.; Liu, H. J.; Guo, F. Q. *J. Nucl. Med.* **2007**, *48*, 2028.
(22) Katz, E.; Willner, I. *Angew. Chem., Int. Ed.* **2004**, *43*, 6042.
(23) Climent, E.; Martinez-Manez, R.; Sancenon, F.; Marcos, M. D.; Soto, J.; Maquieira, A.; Amoros, P. *Angew. Chem., Int. Ed.* **2010**, *49*, 7281.
(24) Niu, D. C.; Ma, Z.; Li, Y. S.; Shi, J. L. *J. Am. Chem. Soc.* **2010**, *132*, 15144.
(25) Slowing, I.; Trewyn, B. G.; Lin, V. S. Y. *J. Am. Chem. Soc.* **2006**, *128*, 14792.
(26) Liu, R.; Zhang, Y.; Zhao, X.; Agarwal, A.; Mueller, L. J.; Feng, P. Y. *J. Am. Chem. Soc.* **2010**, *132*, 1500.
(27) Liu, R.; Zhao, X.; Wu, T.; Feng, P. Y. *J. Am. Chem. Soc.* **2008**, *130*, 14418.
(28) Vivero-Escoto, J. L.; Slowing, I. I.; Wu, C. W.; Lin, V. S. Y. *J. Am. Chem. Soc.* **2009**, *131*, 3462.
(29) Trewyn, B. G.; Slowing, I. I.; Giri, S.; Chen, H. T.; Lin, V. S. Y. *Acc. Chem. Res.* **2007**, *40*, 846.
(30) Dong, H. F.; Lei, J. P.; Ju, H. X.; Zhi, F.; Wang, H.; Guo, W. J.; Zhu, Z.; Yan, F. *Angew. Chem., Int. Ed.* **2012**, *51*, 4607.
(31) Morin, G. B. *Cell* **1989**, *59*, 521.
(32) Slowing, I. I.; Vivero-Escoto, J. L.; Wu, C. W.; Lin, V. S. Y. *Adv. Drug Delivery Rev.* **2008**, *60*, 1278.